

Hyper-thermal stability and unprecedented re-folding of solvent-free liquid myoglobin

Alex P. S. Brogan^a, Giuliano Siligardi^b, Rohanah Hussain^b, Adam W. Perriman^{a,*} and Stephen Mann^a.

^aCentre for Organized Matter Chemistry, School of Chemistry, University of Bristol, Bristol BS8 1TS, UK, and

^bDiamond Light Source, Harwell Science and Innovation Campus, Didcot, Oxfordshire, OX11 0DE, UK

*To whom correspondence should be addressed. E-mail: chawp@bristol.ac.uk

1. SI Methods

Denaturation studies.

Equilibrium thermal denaturation experiments on aqueous solutions of met-Mb, C-Mb or [C-Mb][S₂] were conducted over a temperature range of 25 to 95°C at an average ramp rate of 0.5°C min⁻¹. For CD spectroscopy experiments, the ellipticity at 222 nm was recorded at 1°C intervals followed by a full spectrum scan at every 5°C. For UV-vis spectroscopy, full spectra were recorded every 5°C after a 10 minute equilibration period. Thermal denaturation experiments were also conducted on aqueous solutions (0.1-0.2 mg mL⁻¹) of met-Mb or C-Mb containing the chemical denaturant guanidine hydrochloride (1.5 – 2.5 M). Similar experiments with aqueous [C-Mb][S₂] were unsuccessful due to dissociation of the polymer-surfactant coronal layer by charge screening, and corresponding studies in the presence of urea showed virtually no effect on the thermal unfolding curves, suggesting that the aqueous construct was stabilized against chemical denaturation. For solvent-free liquid [C-Mb][S₂], samples were measured using SRCD spectroscopy from 25 to 225°C at 10°C intervals with an equilibration time of 5 minutes, and from 25 to 175°C using DR-UV-vis spectroscopy at a ramp rate of 10°C min⁻¹ with 5°C intervals and with an equilibrium time of 10 minutes. Thermodynamic parameters were determined according to established procedures assuming a two-state model of thermal denaturation.

Thermal denaturation thermodynamics. Thermodynamic parameters were evaluated by applying a two-state model to the thermal denaturation data¹⁻⁴, which describes the equilibrium between the native state (*N*) and the denatured state (*D*) where the population of each state is defined by the equilibrium constant (*K_D*):



To calculate the position on the equilibrium thermal denaturation pathway, the intensity of the negative circular dichroic peak at 222 nm was used as an order parameter (*y*) to express the fraction denatured (*f_D*),

$$f_D = \frac{(y - y_N)}{(y_D - y_N)} \quad (2)$$

where y_N is defined as the intensity of the 222 nm peak in the native state, and y_D is the intensity of the 222 nm peak in the denatured state. Hence, the fraction denatured can now be used to define the equilibrium constant of denaturation,

$$K_D = \frac{f_D}{1 - f_D} \quad (3)$$

and accordingly, the Gibbs free energy of denaturation (ΔG_D) can be evaluated from the equilibrium constant:

$$\Delta G_D = -RT \ln K_D \quad (4)$$

ΔG_D was plotted as a function of temperature and the transition region was fitted using linear regression. From this curve the half-denaturation temperature (T_m) was evaluated using the x -axis intercept ($\Delta G_D = 0$) and the entropy (ΔS_m) and enthalpy (ΔH_m) at the half-denaturation temperature were evaluated from the gradient of the linear transition region and the product of the half-denaturation temperature (T_m) and entropy (ΔS_m) respectively:

$$\Delta G_m = 0 = \Delta H_m - T_m \Delta S_m \quad (5)$$

Tandem chemical and thermal denaturation thermodynamics.

Thermal denaturation of aqueous C-Mb was not complete at 95°C, and hence it was necessary to use both temperature and guanidine hydrochloride (GndHCl) to yield a series of complete denaturation curves. To improve the accuracy of the analysis, the pre- and post-transition baselines were corrected using:

$$y_N = a_N + b_N T \quad (6)$$

$$y_D = a_D + b_D T \quad (7)$$

For each denaturation curve (corresponding to a given concentration of GndHCl), ΔG_D was evaluated using equations (2) – (4) and plotted as a function of temperature (**Fig. SI Methods 1**), to yield T_m , ΔS_m and ΔH_m , and these values were plotted as a function of denaturant concentration and extrapolated to zero denaturant concentration using linear regression^{5, 6} (**Fig. SI Methods 2**).

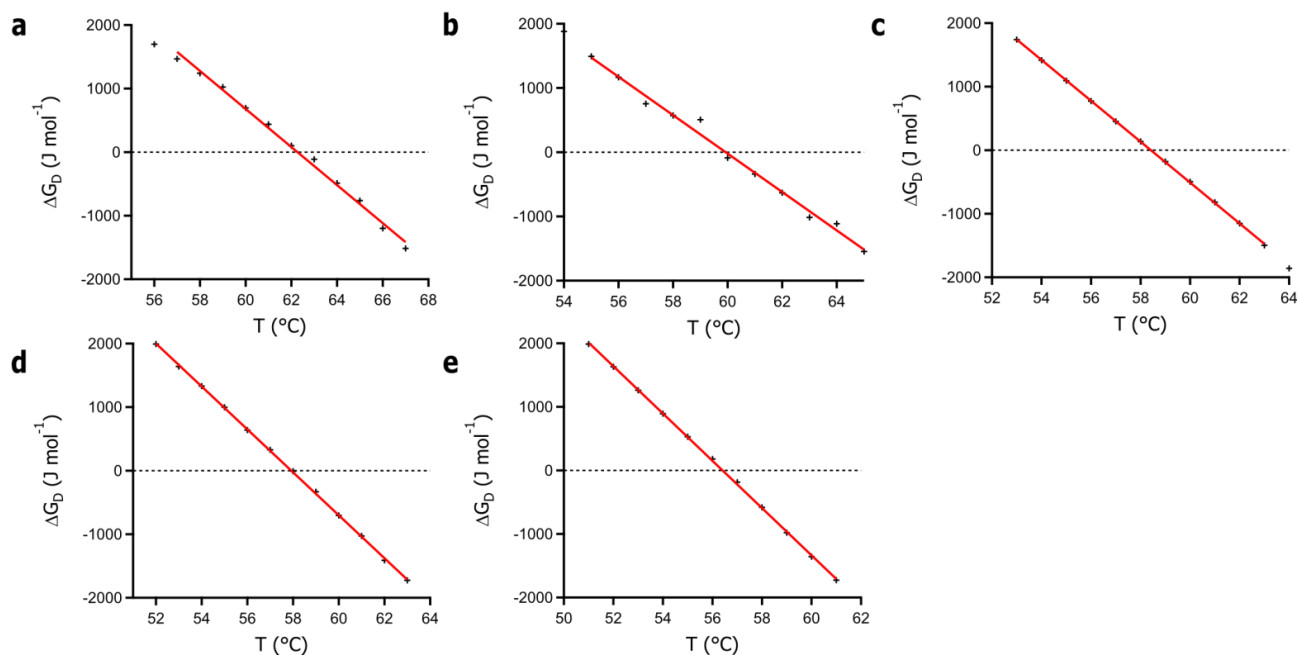


Fig. SI Methods 1. Plots of free energy of denaturation (ΔG_D) as a function of temperature for cationized myoglobin (C-Mb) in the presence of guanidine hydrochloride at 1.5 M (a), 1.8 M (b), 1.8 M (c), 2.0 M (d), and 2.2 M (e).

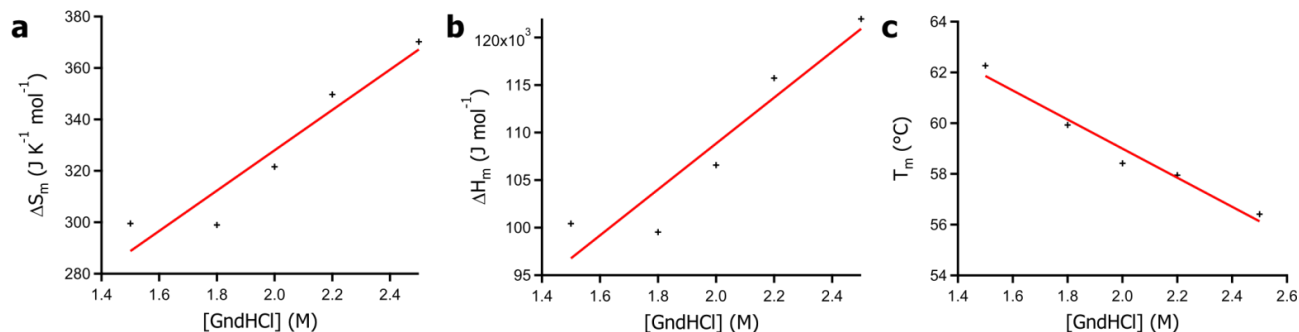


Fig. SI Methods 2. Plots of the entropy of denaturation (ΔS_m) (a), the enthalpy of denaturation (ΔH_m) (b), and the half-denaturation temperature (T_m) (c), of cationized myoglobin (C-Mb) as a function of guanidine hydrochloride concentration.

References

1. C. N. Pace, *Crit. Rev. Biochem.*, 1975, **3**, 1-43.
2. F. Ahmad, *J. Iran. Chem. Soc.*, 2004, **1**, 99-105.
3. S. Taneja and F. Ahmad, *Biochem.J.*, 1994, **303**, 147-153.
4. A. Sinha, S. Yadav, R. Ahmad and F. Ahmad, *Biochem.J.*, 2000, **345**, 711-717.
5. C. M. Johnson and A. R. Fersht, *Biochemistry*, 1995, **34**, 6795-6804.
6. W. Pfeil and P. L. Privalov, *Biophys. J.*, 1976, **4**, 33-40.

2. SI Figures

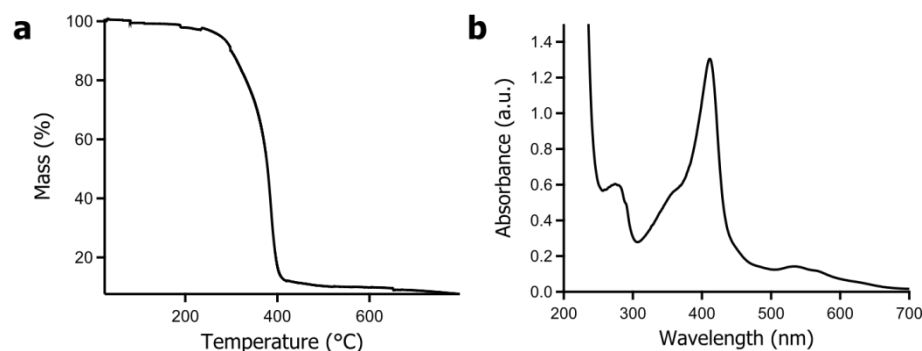


Fig. S1. (a) Thermogravimetric analysis (TGA) of solvent-free liquid [C-Mb][S₂] from 25°C-800°C showing a decomposition temperature of 386°C. The weight loss between 80 and 120°C was 0.23% corresponding to a water content of 6 H₂O molecules per protein. (b) UV-vis spectrum from solvent-free liquid [C-Mb][S₂] after dissolution of a known mass in water to give a total concentration (polymer surfactant plus protein) of 1.06 mg mL⁻¹. The absorption at 280 nm gave a myoglobin concentration of 0.39 mg mL⁻¹, leaving a residual polymer surfactant concentration of 0.67 mg mL⁻¹, which equated to 42 surfactant molecules per protein.

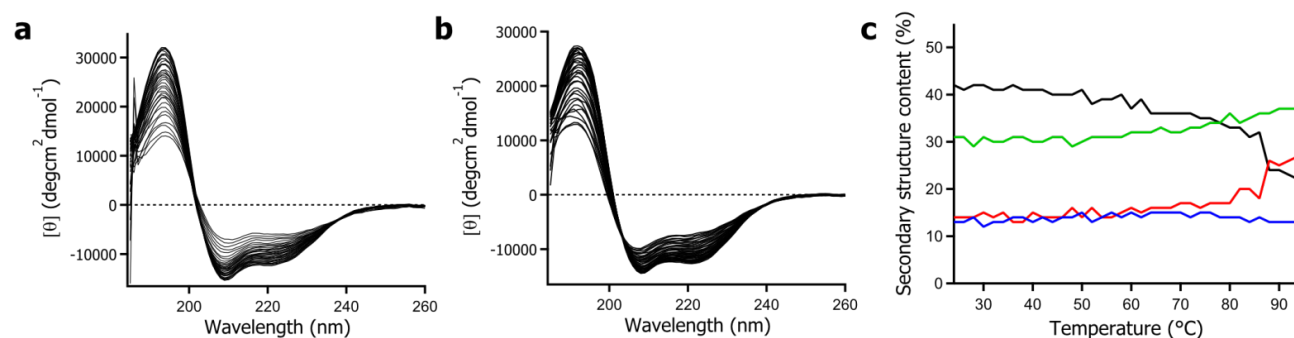


Fig. S2. (a) SRCD spectra from the aqueous nanoconjugate [C-Mb][S₂] showing a reduction in the 195, 208, and 222 nm peak intensities as the temperature was increased from 25°C to 95°C in 2°C intervals. (b) SRCD spectra from aqueous C-Mb showing a reduction in the 195, 208, and 222 nm peak intensities as the temperature was increased from 25°C to 95°C in 2°C intervals. (c) Temperature-dependent changes in the distribution of α-helices (black), β-sheets (red), turns (blue), and unordered (green) domains in aqueous C-Mb.

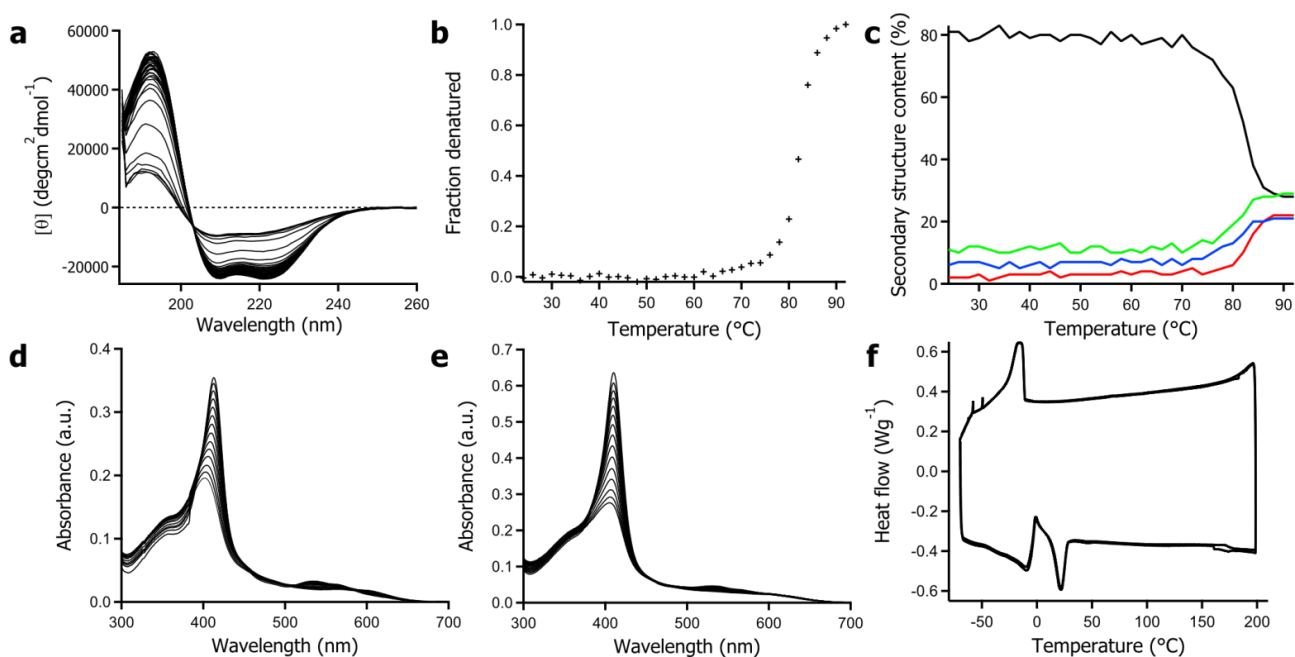


Fig. S3. (a) SRCD spectra from aqueous met-Mb showing a reduction in the 195, 208, and 222 nm peak intensities as the temperature was increased from 25°C to 95°C in 2°C intervals. (b) Plot of fraction denatured against temperature as calculated from (a) using intensity at 222 nm as an order parameter with linear baseline corrections (see equations 2, 6 and 7 SI Methods). (c) Temperature-dependent changes in the distribution of α -helices (black), β -sheets (red), turns (blue), and unordered (green) domains in aqueous met-Mb. (d) UV/Vis spectra from the aqueous nanoconjugate [C-Mb][S₂] showing a reduction in intensity and a blue-shift in the Soret as the temperature was increased from 25 to 95 °C. (e) UV/Vis spectra from aqueous C-Mb showing a reduction in intensity and a blue-shift in the Soret as the temperature was increased from 25 to 95°C. (f) DSC trace from the solvent-free [C-Mb][S₂] liquid showing the endothermic melting transition at 22°C.

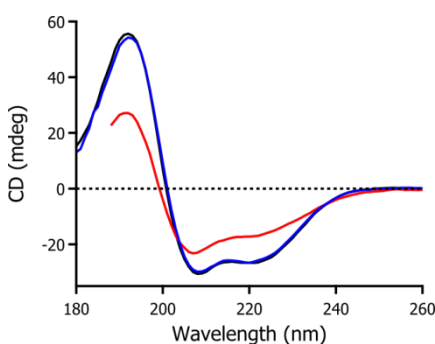


Fig. S4. CD spectra showing the thermal refolding of C-Mb in solution as the temperature is raised from 25°C (black) to 95°C (red), and then returned to 25°C (blue). Samples were incubated for 10 minutes at each temperature.